A Compact Approach for Emotional Assessment of Drone Pilots using BCI.

J. Daniel Olivares-Figueroa, Israel Cruz-Vega, J. M. Ramírez-Cortés, P. Gómez-Gil, and J. Martínez-Carranza
Instituto Nacional de Astrofísica, Óptica y Electrónica (INAOE), Puebla, México

ABSTRACT

In this study, a method based on a *Brain-Computer Interface* (BCI) is proposed to continuously monitor emotional states related to the performance of drone pilots. As part of the contributions of this work, it is the creation of a database to classify two states: *Quiet* and *Very Tense*. The experiments were performed in a simulated environment. The EEG data of each participant was acquired using an EMOTIV Insight headset with 5 EEG channels. We propose an algorithm for automatic real-time artifact removal for five channels as a quick alternative. The *Asymmetry Index* (AI) is proposed as the main feature extracted from the frontal and temporal regions of the brain, followed by statistical measurements calculated from the AI vector to classify the signals with standard classifiers: *K-Nearest Neighbors* (KNN) and *Support Vector Machine* (SVM). We found clear evidence that the AI calculated in the frontal and temporal lobes of the brain is related to the response in drone pilots under emotional tension.

1 INTRODUCTION

Recently, drones for different applications such as civil and military service have increased, including maritime, space missions, search-rescue, shipping-delivery, etc. [1]. Despite being one of the most versatile tools, there are not enough studies that specifically focus on measuring the emotional state of drone pilots during the handling of unexpected emergencies.

Drone pilots engaged in long working hours manifest acute stress, which in the long term can turn into perceived stress [2], especially under adverse environmental conditions [3].

There are different methods for measuring human stress. Subjective methods use questionnaires [4], while objective methods use physical measures, for example facial expressions and blinking frequency, physiological processes, for example measuring the level of adrenaline in the blood, or using biosensors measuring the heart rate, brain waves, among others [2].

Neuroscience has shown that the response of human brain is affected by stress. Non-invasive technologies such as fMRI [5], [6], and *Electroencephalography* (EEG) [7] are the most common sources to study brain activity. However, EEG is a preferred application due to technological advances and commercial availability.

In this study, we propose a method based on a *Brain-Computer Interface* (BCI) to continuously monitor emotional states related to the performance of drone pilots, such as stress, fatigue, attention, and mental workload levels. We compute the *Asymmetry Index* (AI) [7] of the Alpha and Beta rhythms on frontal and temporal regions. The experiments were performed in a simulated environment under controlled conditions, obtaining eight statistical measurements to characterize the AI vector: *mean*, *median*, *standard deviation*, *RMS*, *peak-to-RMS*, *peak-to-peak*, *mean frequency*, and *power*. The proposed system employs these characteristics to train two classifiers: *K-Nearest Neighbors* (KNN) [8] and *Support Vector Machine* (SVM) [9]. The performance is evaluated using the average of *accuracy*, *precision*, *sensitivity*, and *specificity* [10].

To assess our model, a database was generated, which is divided into three classes: *Quiet*, *Tense*, and *Very Tense*. For the experiments presented here, we select the *Quiet* and *Very Tense* groups for the classification process.

The rest of this paper is structured as follows: Section 2 presents the relevant related work to this project. The database generation and its processing are presented in Sections 3 and 4, respectively. Results are shown in Section 5, and finally, the conclusion are presented in Section 6.

2 RELATED WORK

Emotions have a strong correlation with the left and right frontal lobes activity. Stronger activation in the left lobe is related to positive emotions. Instead, when the activation of the right lobe is relatively more significant, it represents mainly negative emotions [11], [2].

Numerous studies show clear evidence that frontal asymmetry is related to emotional responses and

*Email address(es): daniel_olfi@inaoep.com

disorders. Theoretical background can be consulted in reference [12].

Studies related to the detection of stress suggest that frontal asymmetry is a promising biomarker. In [13], a method for identification of chronic stress is presented, finding that the average AI of the stressed group was lower than the group in relaxed condition. A similar result was found by [14], [15], where alpha and beta power asymmetry were analyzed. Low beta waves were analyzed in [4] to quantify human stress, using a single frontal channel efficiently. In [7], shows that the average alpha, beta, and gamma wave AI tends to be lower in the stressed group than in the controlled group and suggests that alpha asymmetry is the best candidate. The calculation of AI on alpha and beta regions reported in this work is based on [7].

3 DATABASE CREATION

Three healthy male volunteers participated in this experiment, with ages between 18 to 23 years old. One subject showed a high level of skills for video games, and the remaining two showed a moderate level; none of the participants had experience in handling drones. Data were acquired between 3 and 6 pm by the three participants.

The EEG data of each participant was acquired with an EMOTIV Insight headset with 5 EEG electrodes (AF3, AF4, T7, T8, Pz) and two reference electrodes (CMS/DRL) located in the left mastoid bone. A data transmission rate of 128 samples per second was used, with a passband of 0.5 to 43 Hz and a notch filter at 50 and 60 Hz (https://www.emotiv.com/insight/).

A database was generated with information obtained from the subjects in three emotional states: *Quiet*, *Tense*, and *Very Tense*. In addition, *Quiet* and *Very Tense* conditions have been used for classification.

3.1 Complementary Information

For each participant, we collect name, age, gender, experience level with video games or drone driving, time of experience, and relevant medical conditions such as injuries, surgeries, chronic diseases, and allergies.

3.2 Experimental Development Environment

In the experiment, we employed two screens, shown in figure 1. First, the operator controlled the experiment using a Graphical User Interface (GUI), label in the figure as "first screen," which is linked to an application provided by EMOTIV Insight developers, called EmotivPRO. Then, using the GUI labeled in figure 1 as "second screen," the participant fulfilled the tasks assigned on each test.

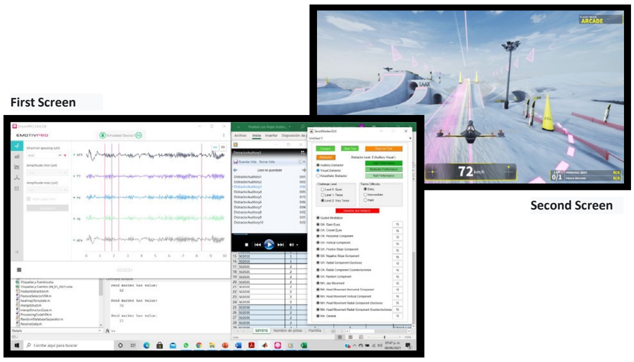

Figure 1: Experimental development environment. Screen for the operator (left) and for the participant (right).

3.3 Practice with the Flight Simulator

A preliminary training session allowed each participant to become familiar with the drone flight simulator and the control commands.

3.4 Recording Calibration Signals

Signals correlated with noise generated by different artifacts, as well as a baseline, were measured. Each subject listened a guided meditation audio for 5 minutes to induce a state of relaxation. Subsequently, each subject followed the instructions shown on the screen to measure ocular and muscular artifacts (eyes open, eyes closed, and movements in all directions of the jaw, neck, and eyes).

3.5 Experimental Tests

Each participant completed different challenges in the "*DCL the Game*" flight simulator (https://dcl.aero/), such as following trajectories and overcoming obstacles on each runway, to test precision and concentration skills. The tracks sizes range from 30 sec to 2 min, depending on the circuit and the pilot's skill in each test. Each session was applied on different days lasting from 25 min to 35 min and exposing the participants gradually to three stress levels: *Quiet*, *Tense*, and *Very Tense* (see Figure 2).

Figure 2: General scheme of a session. Green, yellow, and red blocks for *Quiet*, *Tense*, and *Very Tense* states, respectively. The solid lines joining each block correspond to a 30-seconds break.

Level 0 (Quiet): The participant performs basic maneuvers, such as taking off, landing, turning right, left, moving forward, and backward without obstacles.
Level 1 (Tense): The participant must run each track with obstacles without suffering an accident with the drone. The subjects are instructed to complete the tracks trying to beat his own record in time. The signals obtained from

each track are recorded and stored in the database. In addition, the subject was immersed in music of action and related genres to induce a more significant engagement.

Level 2 (Very Tense): The participant must fulfill the same tasks as Level 2, while being distracted with *auditory* and *visual* stimuli. *Auditory distractors* consisted of sudden, short-lived audios. *Visual distractors* consisted of randomly appearing images, blocking partial vision at different sizes and positions on the screen.

Signals have been labeled and organized according to the following characteristics: Emotional Tension Level, Track Difficulty, Distractors, Pilot Performance, and Test Start/End. In turn, each characteristic can assume one of three possible levels.

4 PROCESSING

Signals classification must perform as a real-time application. Therefore, there is a trade-off between efficiency and speed throughout the entire process. Figures 3, 4, and 5 show the algorithm proposed for real-time signal processing: *Detrend and Artifact Removal*, *Brain Rhythm Filter*, *Asymmetry Index Calculation*, *Feature Extraction*, *Model Training and Testing*.

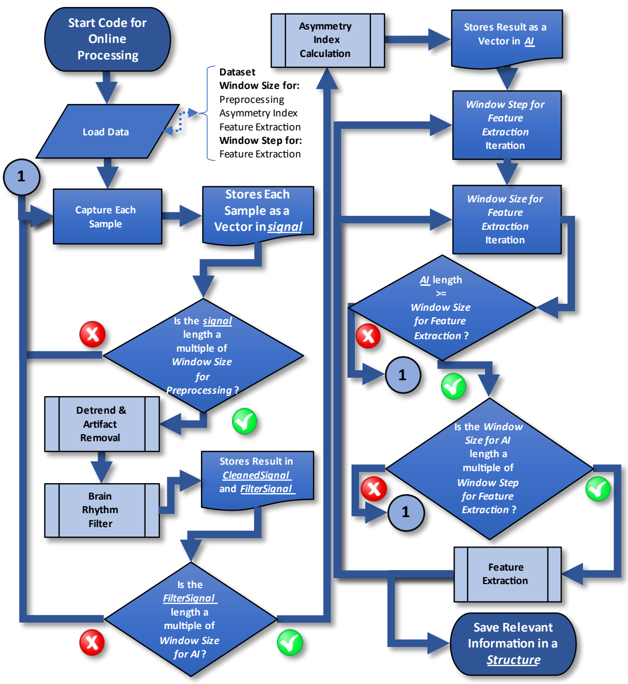

Figure 3: Flowchart proposed for real-time signal processing.

4.1 *Detrend and Artifact Removal*

To detrend and remove the DC component of each EEG channel, we applied *Empirical Mode Decomposition* (EMD) [16], reconstructing the signals by omitting the three lowest frequencies, using the *Intrinsic Mode Functions* (IMF).

Several studies that show sophisticated techniques for artifact removal are limited to offline systems [17], [18]. On the other hand, studies that eliminate artifacts in real-time use 32 or 64 channels [19], focusing on eliminating a single artifact [20], [21], or using a reference signal [22].

We propose an algorithm, inspired in the works of [23] and [19], for automatic real-time artifact removal using five channels. Our aim is to avoid complex approaches proposing a practical and quickly applied alternative. Figure 4 shows the general process.

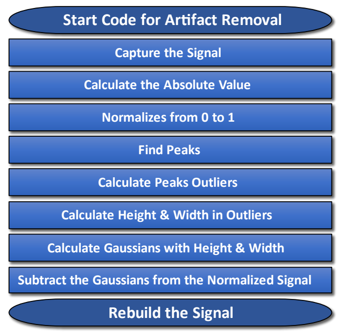

Figure 4: Proposed algorithm for automatic removal of artifacts in real-time.

4.2 *Brain Rhythm Filter*

We designed two cascade IIR filters (high pass filter - low pass filter) Chebyshev Type II of minimum order to extract the Alpha (7-12 Hz) and Beta (12-30 Hz) rhythm. Both were applied using an attenuation in the rejection band of 60 dB per decade.

4.3 *Asymmetry Index Calculation*

The Alpha and Beta *Asymmetry Index* (AI) were calculated using equations (1), (2) and (3), as described in [7] and [24], and stored as a vector. Where AI_f, AI_t and AI, represent frontal, temporal, and total asymmetry, respectively. P_{AF4}, P_{AF3}, P_{T8} and P_{T7} represent the power of the corresponding channel for the rhythm of interest.

$$AI_f = \frac{P_{AF4} - P_{AF3}}{P_{AF4} + P_{AF3}} \quad (1)$$

$$AI_t = \frac{P_{T8} - P_{T7}}{P_{T8} + P_{T7}} \quad (2)$$

$$AI = AI_f + AI_t \quad (3)$$

4.4 *Feature Extraction*

Eight features (*mean*, *median*, *standard deviation*, *RMS*, *peak-to-RMS*, *peak-to-peak*, *mean frequency* and *power*) have been extracted from the asymmetry vector AI_f, AI_t y AI, giving a total of 24 for each rhythm.

4.5 Model Training and Testing

Several models are trained for each step and window size. In each execution (*Run Number*) the training set (80%) and test set (20%) are randomly selected, and different hyper-parameters were tested depending on the type of classifier. For the KNN classifier, distance type (*euclidean*, *seuclidean*, *cityblock*, *minkowski*, *chebyshev*, *cosine*, *correlation*, *spearman*) and K number of nearest neighbors (from 3 to 10) were iterated. For SVM, we used Kernel functions *linear*, *quadratic*, *cubic polynomial*, and *Gaussian* with a Kernel scale of 1.2, 4.9, and 20.

For each execution and iteration of hyper-parameters, models are evaluated in their training and testing stage with *accuracy*, *precision*, *sensitivity*, and *specificity* [10]. Finally, the mean of the four metrics was calculated to select the KNN and SVM hyperparameters with the best average for each step and window size (see figure 5).

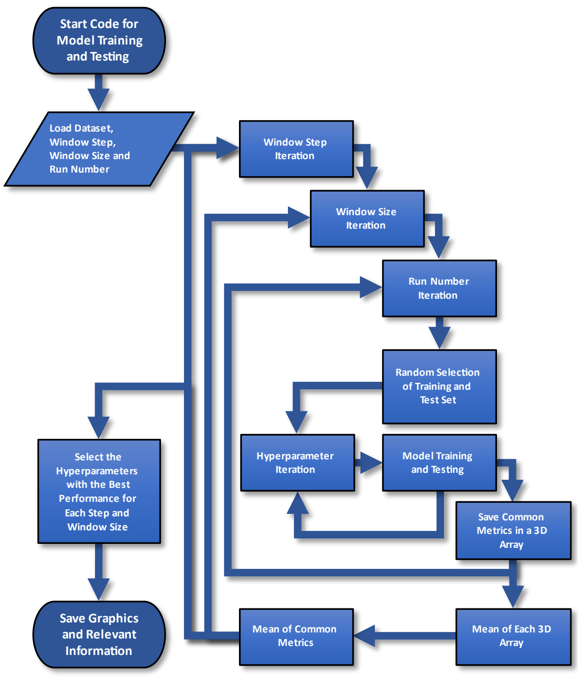

Figure 5: Process for training and testing all models.

5 RESULTS AND DISCUSSIONS

The dataset used in the process described in figure 3 contains the data obtained from the tests applied to each subject. Preprocessing the signal and the calculation the AI were performed using a window of 2 seconds. Four window sizes of 30, 60, 90 and 120 s were considered to extract features. Three window shifts for feature extraction (see figure 3) were tested: 10, 20 and 30 s. The process shown in Figure 5 for the evaluation of the models during training and testing stage was repeated 20 times (*Run Number = 20*). Figures 6, 7 and 8 show the results obtained for each combination of step and window size. These correspond to the best average (in percentage) obtained from the four metrics (*accuracy*, *precision*, *sensitivity,* and *specificity*) at the test stage.

It is observed for all subjects that, regardless of the window step considered, the results tend to improve as the window size increases. The best performance for all three subjects is typically obtained when the window step is 10 s for both classifiers. We can see that the results are very similar among the classifiers.

Comparing the alpha and beta rhythms of the different steps and window sizes for each subject separately, we generally observe that the beta rhythm is higher than the alpha rhythm.

Tables 1 and 2 show the best results and the hyperparameters calculated in both classifiers for alpha and beta rhythms, respectively. We observe that for the KNN classifier, the best results are obtained using 3, 4 and 5 nearest neighbors. This favors the real-time application objective of our study, since the smaller the number of nearest neighbors, the shorter the time required for classification.

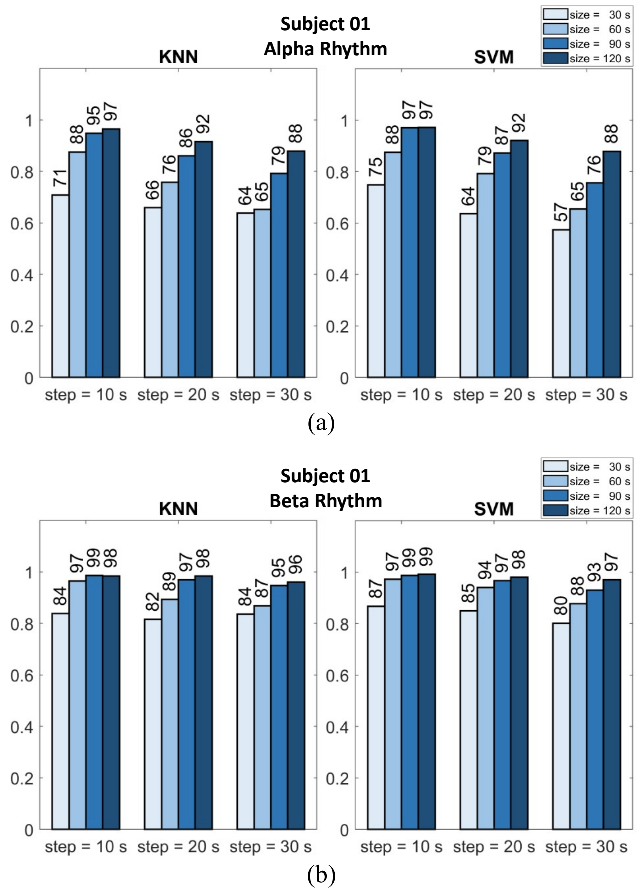

Figure 6: Subject 01. Mean of the metrics for the KNN and SVM classifiers of the (a) Alpha and (b) Beta rhythms.

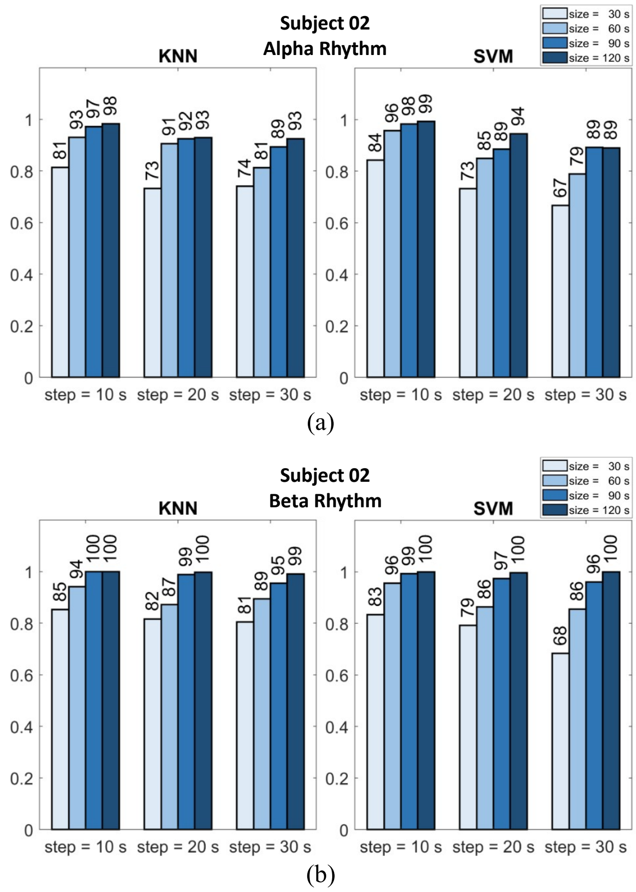

Figure 7: Subject 02. Mean of the metrics for the KNN and SVM classifiers of the (a) Alpha and (b) Beta rhythms.

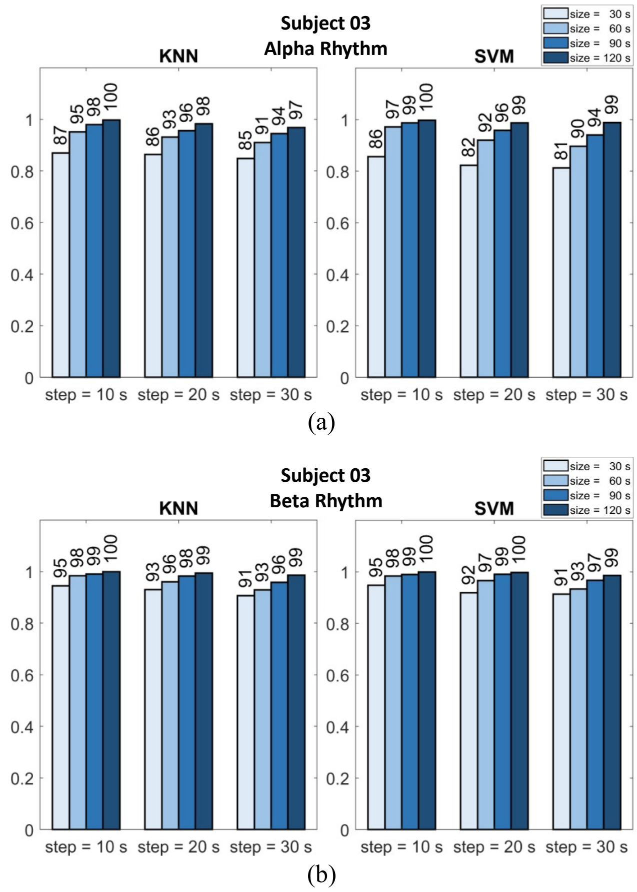

Figure 8: Subject 03. Mean of the metrics for the KNN and SVM classifiers of the (a) Alpha and (b) Beta rhythms.

Alpha Rhythm

	Window		KNN		SVM	
	Step	Size	Metrics Average (%)	Hyper - parameters	Metrics Average (%)	Hyper - parameters
Subject 01	10	90			97	Polynomial Cubic
	10	120	97	Seuclidean K = 4	97	Polynomial Cubic
Subject 02	10	120	98	Cityblock K = 3	99	Polynomial Cubic
Subject 03	10	120	100	Cityblock K = 3	100	Polynomial Cubic

Table 1: Best results obtained for the alpha rhythm.

Beta Rhythm

	Window		KNN		SVM	
	Step	Size	Metrics Average (%)	Hyper - parameters	Metrics Average	Hyper - parameters
Subject 01	10	90	99	Euclidean K = 3	99	Fine Gaussian
	10	120			99	Polynomial Quadratic
Subject 02	10	90	100	Cityblock K = 3		
	10	120	100	Minkowski K = 5	100	Polynomial Quadratic
	20	120	100	Seuclidean K = 5	100	Medium Gaussian
	30	120			100	Polynomial Cubic
Subject 03	10	120	100	Minkowski K = 3	100	Polynomial Quadratic
	20	120			100	Polynomial Quadratic

Table 2: Best results obtained for the beta rhythm.

6 CONCLUSIONS AND FUTURE WORK

In this study, a method is proposed using a BCI to continuously monitor emotional states, which is related to the performance of drone pilots. We built a database to obtain three emotional states where *Quiet* and *Very Tense* states were classified using KNN and SVM. Our findings show that there is a clear separability between these two groups. We proposed an algorithm for automatic real-time artifact removal for five channels as a fast alternative.

We found that the AI in the Alpha and Beta waves is an excellent feature related to the emotional response in drone pilots in situations of emotional tension. Our study suggests that the results corresponding to the four metrics reported in figures 6, 7 and 8 indicate a better performance when the beta rhythm is used, in comparison to those obtained from the alpha rhythm.

Our next step is to expand the database, to test the generalization ability of our model. This database will be publicly available. Also, we will explore other classifiers techniques such as neural networks based on *Deep Learning*.

REFERENCES

[1] M. Hassanalian and A. Abdelkefi, "Classifications, applications, and design challenges of drones: A review," *Prog. Aerosp. Sci.*, vol. 91, no. April, pp. 99–131, 2017, doi: 10.1016/j.paerosci.2017.04.003.

[2] A. Arsalan, M. Majid, A. R. Butt, and S. M. Anwar, "Classification of Perceived Mental Stress Using A Commercially Available EEG Headband," *IEEE J. Biomed. Heal. Informatics*, vol. 23, no. 6, pp. 2257–2264, 2019, doi: 10.1109/JBHI.2019.2926407.

[3] A. Valenzano *et al.*, "Stress profile in remotely piloted aircraft crewmembers during 2 h operating mission," *Front. Physiol.*, vol. 9, no. MAY, pp. 1–6, 2018, doi: 10.3389/fphys.2018.00461.

[4] S. M. U. Saeed, S. M. Anwar, and M. Majid, "Quantification of human stress using commercially available single channel EEG Headset," *IEICE Trans. Inf. Syst.*, vol. E100D, no. 9, pp. 2241–2244, 2017, doi: 10.1587/transinf.2016EDL8248.

[5] K. S. Hong, M. J. Khan, and M. J. Hong, "Feature Extraction and Classification Methods for Hybrid fNIRS-EEG Brain-Computer Interfaces," *Front. Hum. Neurosci.*, vol. 12, no. June, pp. 1–25, 2018, doi: 10.3389/fnhum.2018.00246.

[6] F. Dehais *et al.*, "Monitoring Pilot's Cognitive Fatigue with Engagement Features in Simulated and Actual Flight Conditions Using an Hybrid fNIRS-EEG Passive BCI," *Proc. - 2018 IEEE Int. Conf. Syst. Man, Cybern. SMC 2018*, pp. 544–549, 2019, doi: 10.1109/SMC.2018.00102.

[7] S. M. U. Saeed, S. M. Anwar, H. Khalid, M. Majid, and U. Bagci, "EEG based classification of long-term stress using psychological labeling," *Sensors (Switzerland)*, vol. 20, no. 7, pp. 1–15, 2020, doi: 10.3390/s20071886.

[8] P. E. H. T.M. COVER, "Nearest Neighbor Pattern Classfication," vol. I, pp. 1–28, 2012.

[9] A. Ben-Hur, C. S. Ong, S. Sonnenburg, B. Schölkopf, and G. Rätsch, "Support vector machines and kernels for computational biology," *PLoS Comput. Biol.*, vol. 4, no. 10, 2008, doi: 10.1371/journal.pcbi.1000173.

[10] T. Fawcett, "An introduction to ROC analysis," *Pattern Recognit. Lett.*, vol. 27, no. 8, pp. 861–874, 2006, doi: 10.1016/j.patrec.2005.10.010.

[11] M. Mohammadpour, S. M. R. Hashemi, and N. Houshmand, "Classification of EEG-based emotion for BCI applications," *7th Conf. Artif. Intell. Robot. IRANOPEN 2017*, pp. 127–131, 2017, doi: 10.1109/RIOS.2017.7956455.

[12] J. A. Coan and J. J. B. Allen, "Frontal EEG asymmetry as a moderator and mediator of emotion," *Biol. Psychol.*, vol. 67, no. 1–2, pp. 7–50, 2004, doi: 10.1016/j.biopsycho.2004.03.002.

[13] H. Peng *et al.*, "A method of identifying chronic stress by EEG," *Pers. Ubiquitous Comput.*, vol. 17, no. 7, pp. 1341–1347, 2013, doi: 10.1007/s00779-012-0593-3.

[14] J. W. Ahn, Y. Ku, and H. C. Kim, "A novel wearable EEG and ECG recording system for stress assessment," *Sensors (Switzerland)*, vol. 19, no. 9, 2019, doi: 10.3390/s19091991.

[15] F. Al-Shargie, M. Kiguchi, N. Badruddin, S. C. Dass, A. F. M. Hani, and T. B. Tang, "Mental stress assessment using simultaneous measurement of EEG and fNIRS," *Biomed. Opt. Express*, vol. 7, no. 10, p. 3882, 2016, doi: 10.1364/boe.7.003882.

[16] N. E. Huang *et al.*, "The empirical mode decomposition and the Hubert spectrum for nonlinear and non-stationary time series analysis," *Proc. R. Soc. A Math. Phys. Eng. Sci.*, vol. 454, no. 1971, pp. 903–995, 1998, doi: 10.1098/rspa.1998.0193.

[17] A. Santillan-Guzman, U. Heute, M. Muthuraman, U. Stephani, and A. Galka, "DBS artifact suppression using a time-frequency domain filter," *Proc. Annu. Int. Conf. IEEE Eng. Med. Biol. Soc. EMBS*, pp. 4815–4818, 2013, doi: 10.1109/EMBC.2013.6610625.

[18] A. Santillán-Guzmán, U. Heute, U. Stephani, H. Mühle, A. Galka, and M. Siniatchkin, "Hybrid filter for removing power-supply artifacts from EEG signals," *Proc. IASTED Int. Conf. Biomed. Eng. BioMed 2013*, no. BioMed, pp. 41–45, 2013, doi: 10.2316/P.2013.791-022.

[19] S. Çınar and N. Acır, "A novel system for automatic removal of ocular artefacts in EEG by using outlier detection methods and independent component analysis," *Expert Syst. Appl.*, vol. 68, pp. 36–44, 2017, doi: 10.1016/j.eswa.2016.10.009.

[20] U. Heute and A. S. Guzmán, "Removing 'Cleaned' eye-blinking artifacts from EEG measurements," *2014 Int. Conf. Signal Process. Integr. Networks, SPIN 2014*, pp. 576–580, 2014.

[21] X. Jiang, G. Bin Bian, and Z. Tian, "Removal of artifacts from EEG signals: A review," *Sensors (Switzerland)*, vol. 19, no. 5, pp. 1–18, 2019, doi: 10.3390/s19050987.

[22] L. Pion-Tonachini, S. H. Hsu, C. Y. Chang, T. P. Jung, and S. Makeig, "Online Automatic Artifact Rejection using the Real-time EEG Source-mapping Toolbox (REST)," *Proc. Annu. Int. Conf. IEEE Eng. Med. Biol. Soc. EMBS*, vol. 2018-July, pp. 106–109, 2018, doi: 10.1109/EMBC.2018.8512191.

[23] P. Li, Z. Chen, and Y. Hu, "A method for automatic removal of EOG artifacts from EEG based on ICA-EMD," *Proc. - 2017 Chinese Autom. Congr. CAC 2017*, vol. 2017-Janua, pp. 1860–1863, 2017, doi: 10.1109/CAC.2017.8243071.

[24] E. Baehr, J. Peter Rosenfeld, R. Baehr, and C. Earnest, "Comparison of two EEG asymmetry indices in depressed patients vs. normal controls," *Int. J. Psychophysiol.*, vol. 31, no. 1, pp. 89–92, 1998, doi: 10.1016/S0167-8760(98)00041-5.